Humidity sensor failure: a problem that should not be neglected by the numerical weather prediction community

Yan Liu[1, 2] and Nanjun Tang[3]

[1]{Numerical Weather Prediction Center, China Meteorological Administration,No.46 South Zhongguancun Street, Haidian District, Beijing 100081, China}

[2]{National Meteorological Center, China Meteorological Administration, No.46 South Zhongguancun Street, Haidian District, Beijing 100081, China}

[3]{College of Atmospheric Science, Nanjing University of Information Science and Technology,No.219 Ningliu Road, Nanjing,210044, China}

Correspondence to: Yan Liu (liuyan@cma.gov.cn)

Abstract

The problem of the abnormally dry bias induced by the radiosonde humidity sensor failure in the low- and mid-troposphere is studied based on the global operational radiosonde relative humidity observations from December 2008 to November 2009. At the same time the humidity retrieval from Formosa Satellite mission-3/Constellation Observing System for Meteorology, Ionosphere, and Climate (FORMOSAT-3/COSMIC，simply referred to as COSMIC hereafter) in the same period are used to assess the quality of the radiosonde humidity observations. Results show that the extremely dry relative humidity observations are considerably common in the low- and mid-troposphere with the annual global-averaged occurrence of 4.2%. These low humidity observations usually exist between 20° and 40° latitudes in both northern and southern hemispheres, and in the height from 700 to 450 hPa. Winter and spring are the favoured seasons for their occurrence, with the maximum ratio of 9.53% in the northern hemisphere and 16.82% in the southern hemisphere. The phenomenon is not the results of the natural atmosphere variability totally; on the contrary, it may be the result of humidity sensor failure. If the performances of the humidity sensors are not so good, the low humidity observations occur easily, particularly in the environment when the radiosonde balloon goes through the stratiform clouds with high moisture content. The humidity sensor cannot adapt the huge change of the atmospheric environment inside and outside stratiform clouds, resulting in the failure of sensor and stop response the atmospheric change. These extremely dry relative humidity observations are erroneous. But they have been archived as the formal data and applied in the science research. The reliability of numerical weather prediction and the analysis of climate will be doubled, if the quality control is not applied before using these data.

Key words: operational radiosonde system, relative humidity, humidity sensor failure, abnormally dry, low- and mid-troposphere

1 Introduction

Radiosonde observation is an important means of obtaining upper-air temperature, pressure, moisture and wind observation. It has been used operationally for over 70 years. Although the performance of the radiosonde humidity sensor and the accuracy of observational data are gradually being improved, the data quality has not been satisfied, particularly in the upper troposphere and lower stratosphere, wherein the sensor cannot detect the high relative humidity inside cirrus clouds. A number of studies, including the data analysis using the long-term observations, the international inter-comparisons experiments of the different radiosonde system organized by the World Meteorological Organisation (WMO) etc., have demonstrated that the humidity observations have larger errors (Li et al., 2012). These errors are associated with the bad performance of the humidity sensor under low temperature and low humidity conditions, thus resulting in time-lag errors, sensor icing, aging and contamination (Wang et al., 2003; Miloshevich et al., 2006; Vömel et al., 2007; Nash , et al., 2010; Bian et al., 2011). Although radiosonde hygrometers have been updated from gold beater skin hygrometers and carbon-film hygrometers to capacitive hygrometers, the above problems have not been fully solved. Some operational radiosonde hygrometers using carbon hygristors fail to respond the humidity changes in the upper troposphere, even in the middle troposphere sometimes; an example is US Sippican humidity sensor, which may be unresponsive at the height where temperature is only −8 ° C (Wang et al., 2003).

Recently a new issue has been paid attention from Chinese L-band radiosonde relative humidity observations (Tang et al., 2014). The relative humidity profiles often indicate deep dry layers in the lower troposphere, which show low relative humidity values (RHs <2%) at a given height and above, and no response to humidity changes for a long time even to the end of the soundings observation (Figure 1a). Occasionally, some profiles can recover partly or entirely with height (Figure 1b). Although low RHs of less than 10% are common in the troposphere (Spencer and Braswell, 1997; Zhang et al., 2003; Wang et al., 2010), Zhang et al. (2010) suggested that such dramatic changes of the relative humidity from Chinese L-band radiosonde system do not comply with the atmospheric stratification law. Tang et al. (2014) analysed that the dry biases observed in the lower troposphere, and compared the radiosonde humidity profiles with the COSMIC humidity retrievals (Anthes, et al., 2008). They thought that the dry biases are unnatural anomalies. These dry biases would likely be the result of humidity sensor failure, because the sensors entirely stop working at a certain altitude (a random altitude, but quite low). Tang et al. (2013) further showed that the dry bias phenomenon depends on the performance of the humidity sensor and the cloud types encountered by the sensors. The humidity sensor will easily fail if the sounding instrument goes through deep and thick clouds, most of which are stratiformis clouds with high water vapour and an obvious dry layer, and is accompanied by atmospheric temperature stratification.

The occurrence percentage of dry bias in the Chinese L-band radiosonde system due to humidity sensor failure reaches 12.63% in the survey (Tang, et al., 2014). It is a serious problem that should not be neglected by the numerical weather prediction community. Do the relative humidity observations from other countries' operational radiosonde system indicate the abnormal dry phenomenon? If so, what are the causes and what are their characteristics? It is the aim of this paper. The remainder of this paper is organised as follows. Chapter 2 describes the data and methods employed in this study. Chapter 3 details the survey if other operational radiosonde humidity observations also exist the extremely deep dry biases. Chapter 4 presents the comparison between radiosonde relative humidity observations and radio occultation (RO) observations. Chapter 5 shows the possible causes of the relative humidity observation dry biases. Chapter 6 is the conclusion and discussion.

2 Data and method

The radiosonde data used in this paper are between December 2008 and November 2009 and are obtained from the Global Telecommunication System. After excluding the stations with less than 5 observations, a total of 844 radiosonde stations and 451283 data are obtained. The method proposed by Tang et al. (2013) is adopted to survey the dry bias problem of global operational radiosonde relative humidity observations. If a relative humidity profile with a value of less than 5% continuously appears at the range of more than 200 hPa below the 300 hPa height, we assume that the humidity profile exists dry bias caused by the sensor failure. We define the height under 300 hPa, in order to emphasize that it is a new issue of humidity observation in the low and middle troposphere, instead of the well-known old issue of dry bias in the high troposphere.

The RO data of the Constellation Observation System of Meteorology, Ionosphere and Climate (COSMIC) (Anthes et al., 2008) and the analysis results of the European Centre for Medium-Range Weather Forecasts (ECMWF) model at the same time period are used for inter-comparison. The matching method between RO and radiosonde data is same to the method implemented by Tang et al. (2013). The time window for the match is three hours before and after the radiosonde observation time, and the space window is in a 250 km × 250 km square grid at the centre of the radiosonde. If RO falls within the grid, radiosonde matching is confirmed. If multiple RO profiles are matched at the same time, we select the nearest RO profile.

Firstly, the Magnus saturation vapour pressure equation

$$e_s = \begin{cases} 6.112 \times \exp\left(\frac{17.62 \times t}{243.12 + t}\right) \times F(p) & if\,(t \geq -45) \\ 6.112 \times \exp\left(\frac{22.46 \times t}{272.62 + t}\right) \times F(p) & if\,(t < -45) \end{cases} \quad (1)$$

is used to calculate the saturation vapour pressure of the RO observation. Vapour pressure is then converted to relative humidity, where t represents the temperature in °C, and F (p) is the enhancement factor related to atmospheric pressure:

$$F(p) = 1.0016 + 3.15 \times 10^{-6} \times p - \frac{0.074}{p}, \quad (2)$$

$$RH = \frac{e}{e_s} \times 100\%. \quad (3)$$

To compare these data, we must convert the radiosonde data from a geopotential height to a geometric height coordinate by using the following equation:

$$z = \frac{a \times \bar{g} \times z_g}{g_0(\varphi,0) \times a - \bar{g} \times z_g}, \quad (4)$$

where Z represents the geometric height, Z_g represents the geopotential height, a is the radius of the Earth at 6371 km, $\bar{g} = 9.80655$ m/s2, which is the average at a 45° latitude at sea level, $g_0(\varphi,0)$ is the acceleration of gravity at latitude φ at sea level and

$$g_0(\varphi,0) = 9.80620 \times (1 - 0.0026442\cos 2\varphi + 0.0000058\cos^2 2\varphi) \quad (5)$$

Finally, we use the cubic spline interpolation method to interpolate the radiosonde data to vertical layers with a resolution of 100 m, same resolution to the RO data.

3 Results

3.1 Global distribution of humidity sensor failures

Table 1 shows the number and ratio of all and failure relative humidity observations for four seasons. A total of 18,609 failure relative humidity observations among 447,021 observations are recorded between December 2008 and November 2009, and the percentage of failure observation is approximately 4.17% worldwide. Table 1 shows that humidity sensor failure can occur at any time but mostly occurs during winter and spring for both hemispheres, with the highest percentage during winter at 9.53% in the mid-latitude region of the northern hemisphere and 16.82% in the mid-latitude region of the southern hemisphere. In the survey, 211 among 844 radiosonde stations have no failure observations; these stations are mainly located in the high-latitude regions of the northern hemisphere and in tropical regions.

Figure 2 shows the number of relative humidity sensor failure observations for each radiosonde station during the period of the survey. Different colour dots correspond to the number presented in the colour bar, and the black hollow circle indicates that no humidity sensor failure is observed. The failure observations mainly occur in the latitudes between 20° and 40° for both hemispheres. The number of failure observations is high in China, the United

States, Australia, Western Europe and the east coast of South America. The problem in China is particularly serious with a maximus of 218 among 720 in Dalian station. However, the humidity sensor failure is rare in the tropical and high-latitude regions.

3.2 Characteristics of seasonal variation and vertical distribution

Figure 3 presents the statistics of relative humidity sensor failure observations for four seasons. As shown in the images, failure relative humidity observations occur mainly during spring and winter. Failure observations are less during the summer, and gradually increase during autumn. This trend is observed near 30° latitudes for both the northern and southern hemispheres.

What is the vertical distribution characteristic of the failure relative humidity observations? Figure 4 shows the height and total station number, which satisfy the failure criterion. The height of most failure observations is between 700 hPa and 450 hPa and peaks at 700 hPa to 650 hPa followed by 500 hPa to 450 hPa. Failure observations may be seen under 900 hPa, which indicates humidity sensor failure may occur in the very low height.

4 Comparison with COSMIC/GPS RO data

Table 2 lists the number of all observations, failure observations and matched failure observations obtained by RO and three widely used operational instruments, namely, Finland's Vaisala, the US Sippican and the Chinese L-band radiosonde system. We calculate the bias and standard deviation for the failure, normal and all observations. Figure 5a shows the statistical results for all sondes in the entire year. Figures 5b-d present the comparison of the results obtained by three instruments with COSMIC/GPS 1Dvar retrieval data. The number of failure observations is small on the global basis, thus resulting in the near superposition of the normal observation line (blue) and all observation line (red). Figure 5a also shows that the bias between normal and all observations is about ±5% under 8 km height; thus, although COSMIC data has an error, the data are still in line with the WMO requirements on observation uncertainty and are suitable for cross-comparison. Compared with RO data, dry bias from failure data is larger than that in normal cases and the Maximus bias is beyond −10%. Figures 5b to 5d shows the similarity between Vaisala, Sippican and L-band humidity sensors to the COSMIC retrieval humidity data. However, the dry bias of Vaisala is smallest, whereas the dry bias of the Chinese L-band is large in the entire troposphere; this result is consistent with other research findings (Li et al., 2009; Sun et al., 2010; Bian et al., 2011).

Figure 6 illustrates two radiosonde relative humidity profiles in comparison with ECMWF analysis and RO data. The radiosonde observation, RO data and analysis generally have good consistency in the normal state. However, at the occurrence of a humidity sensor failure, the relative humidity drops from high moisture to low moisture quickly, and the sensor stops working entirely from a certain altitude. Although the RO and analysis profiles also experience a rapid decrease, the reduction will not be less than 10% and the value will not remain constant, which indicates that temperature, pressure and humidity data based on 1Dvar are not subjected to the sensitivity of the sensors. Sometimes the humidity sensor can partly or fully recover as the balloon re-enters the clouds (Fig. 6b), including cirrus clouds, because the high moisture inside the clouds is helpful for sensor recovery. Figure 6 also illustrates that the abnormal dry phenomenon in the lower troposphere is unreasonable, it does not reflect the true state of the atmosphere. However, these data have been archived as formal records and widely used in scientific research and services. If these data are used without correction and quality control, weather prediction and climate analysis will be significantly affected. RO observations and the analysis of numerical weather prediction might provide an effective approach to correct or remedy the failure radiosonde humidity observations.

5 Possible causes of humidity sensor failure

5.1 Performance of the sensor

Figure 7 shows the relative humidity and temperature profiles of six different failure sensors. As seen in the figures, the relative humidity observations decrease quickly in a short time from a high humidity value to below 5% in the middle-lower troposphere and then maintains low humidity values. For example, the German Graw G sensor decreases rapidly from 93% to

1% from a height of 820 hPa to 787 hPa and then maintains low humidity values. Some sensors lose their sensing ability entirely (Figures 7a and 7d), whereas other sensors may recover. The relative humidity in all cases is over 87%. When the value starts decreasing, an inversion temperature layer is observed, thus revealing the existence of clouds in these cases.

Figure 8 shows the distribution of the operational radiosonde stations worldwide. The different colours represent different humidity sensors. In contrast to Figure 2, we find that all sensors are potential failures and most of them are carbon hygrometers. In the figure, the blue point represents the Vaisala sensor, which is widely used in Western Europe, Australia and South America. Although the Vaisala uses capacitive hygrometers and is recognised the best sensor, the number of failure observations is quite few. Therefore, instrument capability is not the only cause of sensor failure. However, the similarity between Figures 8 and 2 indicates that instrument capability is always an important factor that should not be ignored. The capability of the Chinese L-band system is insufficient; hence, this sensor tends to exhibit significant problems.

5.2 Relationship to the atmospheric condition, especially clouds

Figure 9 presents the distribution of stratiform clouds and their temporal evolvement from the International Satellite Cloud Climatology Plan D2 data sets in the corresponding period. A low cloud belt exists near 30° in the northern and southern hemispheres, which is consistent with Klein's results (1993). From above analysis, the failure relative humidity observations mainly occur at nearby 30° latitude in both hemispheres, and are particularly obvious in winter. Does it imply if there are some connections between the failure of humidity sensor and the distribution of stratiform clouds?

Generally, relative humidity is high inside stratiform clouds and low between two interbeds of clouds; it decreases sharply at the top of clouds. The gradient of temperature stratification is close to that of the wet adiabatic process. The upper and top of the stratiform clouds usually have an inversion temperature layer that appears below the clouds at a height of 0.1 km to 0.2 km away from the top of the clouds (Shi, 2005). The examples provided in Section 5.1 indicate that the relative humidity of all radiosondes is over 87% and decreases sharply with the existence of the inversion temperature layer (Fig. 7). Obviously, it is the phenomenon when the balloon goes out the stratiform clouds.

Wang et al. (2003) suggested that the sensor will lose sensitivity and stop responding in cold temperatures (approximately below −34 °C or above 8.5 km), or when relative humidity significantly changes within a short time. However, they did not analyse why relative humidity dramatically changes within a short time. From above analysis, we think that the dramatic changes of relative humidity occur after the balloon goes through the stratiform clouds, especially the wide range of stratiform clouds. The radiosonde balloon drifts during flying, and the horizontal scale of stratiform clouds is ten to thousands of kilometres, thus resulting that the horizontal distribution of the atmosphere is relatively uniform and stable, but the vertical distribution may exhibit dramatic changes. The horizontal scale of convective clouds is smaller, and the low humidity area is located inside cloud monomers. The balloon may repeatedly go through convective clouds from the sides instead of the tops. Therefore, the temperature and humidity profiles cannot depict the relatively uniform changes in the horizontal and drastic changes in the vertical for convective clouds.

6 Conclusion and discussion

According to the radiosonde data from December 2008 to November 2009, the problem of the abnormally dry bias induced by the radiosonde humidity sensor failure in the low- and mid-troposphere is studied, which has not been paid more attention at present. We calculated the percentage of their occurrence, compared these observations with other satellite products and reanalysis data, and analyzed the possible causes. The main conclusions are as follows:

(1) In the middle and lower troposphere, the deeply dry layer is often observed on the based of the relative humidity observations from the operational radiosonde system. This phenomenon is common. However, it is different from the dry layer in the natural variability, which exist in the troposphere, especially in the subtropics and extratropics based on the previous studies. One of the most obvious features is that the relative humidity in our study has less change with time and has maintained in a very low value in a deep atmospheric layer,

indicating that the hygrometer seems not respond the varation of the atmosphere. Globally, the annual average occurrence percentage of such dry humidity observations is approximately 4.2%, and these observations mainly occur between the height of 700 and 450 hPa at 20° to 40° latitude for the northern and southern hemispheres. The percentage is high, especially in winter, reaching 9.53% in the middle altitudes of northern hemisphere and 16.82% in the middle altitudes southern hemisphere, respectively.

(2) The reasons behind the extremely low relative humidity observations in the low- and middle-troposphere are the performance of the radiosonde humidity sensor and the cloud types in the atmosphere. When the balloon goes through the deep stratiform clouds with high moisture content, due to the huge changes in the external atmospheric conditions, the humidity sensor might be difficult to adapt, then fail and stop responding. The dramatical change of relative humidity in a short time further reveals the possible variation of the atmosphere state. But the internal physical mechanism of the humidity sensor failure is still needed investigation.

(3) The low relative humidity data that satisfy the criteria proposed by Tang et al. (2014) are erroneous. These data do not represent the real atmospheric status. However, they have been archived as formal records, and are widely used in atmospheric science research and services. If the data are used prior to correction and quality control, the reliability of the weather prediction and climate analysis will be significantly doubted. Therefore, there is an urgent need for taking effective measures to correct the erroneous data.

Acknowledgements: This study was supported by the National Science Foundation of China (41075081) and the China Meteorological Administration Special Public Welfare Research Fund (GYHY201106008 and GYHY201206007).

References

Anthes, R. A., Bernhardt, P. A., Chen, Y., Cucurull, L., Dymond, K. F., Ector, D., Healy, S. B., Ho, S. P., Hunt, D. C., Kuo, Y.-H., Liu, H., Manning, K., McCormick, C., Meehan, T. K., Randel, W. J., Rocken, C., Schreiner,W. S., Sokolovskiy, S.V., Syndergaard, S.,Thompson, D. C., Trenberth, K. E., Wee, T. K., Yen, N. L., and Zeng, Z.: The COSMIC/FORMOSAT-3 Mission-Early results, B. Am. Meteorol. Soc., 89, 313–333, 2008.

Bian, J., Chen, H., Vmel, H., Duan, Y., Xuan, Y., and Lv, D.: Intercomparison of humidity and temperature sensors: GTS1, Vaisala RS80, CFH, Adv. Atmos. Sci., 28, 139–146, 2011.

Klein, S. A., Hartmann, D. L.: The seasonal cycle of low stratiform clouds, J. Climate, 6, 1587-1606,1993.

Li, F., Li, B. and Wu, L.: An introduction of WMO 8th radiosondes inter-comparison and integrated remote instruments experiment, Advances in Earth Science, 27,916-924, 2012(in chinese).

Li, W.，Xing, Y.，Ma, Sh. Q.: The analysis and comparison between GTS1 radiosonde made in China and RS92 Radiosonde of Vaisala company, Meteological monthly, 35, 97-102, 2009 (in chinese).

Miloshevich, L. H., Vömel, H., Whiteman, D., Lesht, B., Schmidlin, F. J. and Russo, F : Absolute accuracy of water vapor measurements from six operational radiosonde types launched during AWEX-G and implications for AIRS validation, J. Geophys. Res., 111, D09S10, 2006.

Moradi, I., Buehler, S. A., John, V. O., and Eliasson, S.: Comparing upper tropospheric humidity data from microwave satellite instruments and tropical radiosondes, J. Geophys. Res., 115, D24 310, 2010.

Nash, J., Oakley, T., Vömel, H. and Li, W.: WMO intercomparison of high quality radiosonde systems,World Meteorol. Org., Yangjiang, China, Tech. Rep., 2010.

Shi, A.: Progress in researches on microphysical characteristics and precipitation mechanisms of stratiform cloud precipitation, Meteorological Science and Technology，2, 104-108, 2005 (in chinese).

Spencer, R. W., and Braswell, W. D.: How dry is the tropical free troposphere? Implications for global warming theory, Bull. Amer. Meteor. Soc., 78, 1097–1106, doi:10.1175/1520-0477, 1997.

Sun, B., Reale, A., Seidel, D. J. and Hunt, D. C.: Comparing radiosonde and COSMIC atmospheric profile data to quantify differences among radiosonde types and the effects of imperfect collocation on comparison statistics, J. Geophys. Res., 115, D23104,doi:10.1029，2010JD014457, 2011.

Tang, N., Liu, Y., Li, G. and Li, F. : Preliminary analysis on abnormally dry phenomena of relative humidity observations of the Chinese L-band radiosonde system, Journal of Tropical Meteorology, 30(4), 1004-4965(2014)04-0065-11, 2014 (in Chinese).

Vömel, H., Selkirk, H., Miloshevich, L., Valverde-Canossa, J., Valdés, J., Kyrö, E., Kivi, R., Stolz, W., Peng, G., Diaz, J. A. : Radiation dry bias of the Vaisala RS92 humidity sensor, J. Atmos. Oceanic Technol., 24, 953-963, 2007.

Wang, J. H. and Rossow, W. B.: Determination of cloud vertical structure from upper air observations, J. Appl. Meteor., 34, 2243-2256,1995.

Wang, J. H., Cole, H. L., Carlson, D. J., Miller, E. R., Beierle, K., Paukkunen, A. and Laine, T. K.: Corrections of humidity measurement errors from the Vaisala RS80 radiosonde - application to TOGA COARE data, J. Atmos. Ocean. Technol., 19, 981-1002, 2002.

Wang, J. H., David, J. C., David, B. P., Terrence, F. H., Dean, L., Harold, L. C., Kathryn, B. and Edward, C.: Performance of operational radiosonde humidity sensors in direct comparison with a chilled mirror dew-point hygrometer and its climate implication, Geophys. Res. Lett., 30, 1860,doi:10.1029/2003GL016985,2003.

Wang, J. H., Zhang, L.Y., Lin, P.N., Mark, B., Harold, C., Jack, F., Terry, H., Dean, L., Scot, L., Charlie, M., Joseph, V., Weng, C-H. and Kathryn Y.: Water vapor variability and comparisons in the subtropical Pacific from The Observing System Research and

Predictability Experiment-Pacific Asian Regional Campaign (T-PARC) Driftsonde, Constellation Observing System for Meteorology, Ionosphere, and Climate (COSMIC), and reanalyses，J. Geophys. Res., 115, d21108, doi:10.1029/2010jd014494, 2010.

WMO-NO. Guide to Meteorological Instruments and Methods of Observation, 2008 edition (7TH), Updated in 2010, Geneva, 2012.

Wolfgang, S., Claude, H., Schönenborn, F., Leiterer, U., Dier H. and Lanzinger E.: Pressure and temperature differences between Vaisala RS80 and RS92 radiosonde systems, J. Atmos. Ocean. Technol., 25（6）, 909-927, 2008.

Zhang, C. D., Mapes, B. E., and Soden, B. J.: Bimodality in tropical water vapour, Quart. J. Roy. Meteor. Soc., 129, 2847–2866, doi:10.1256/qj.02.166, 2003.

Zhang, C. and Chen J.: Contrast analysis of data observed by 59-type and L-band sonde，Journal of Shanxi Meteorology, 1, 29-31, 2010 (in chinese).

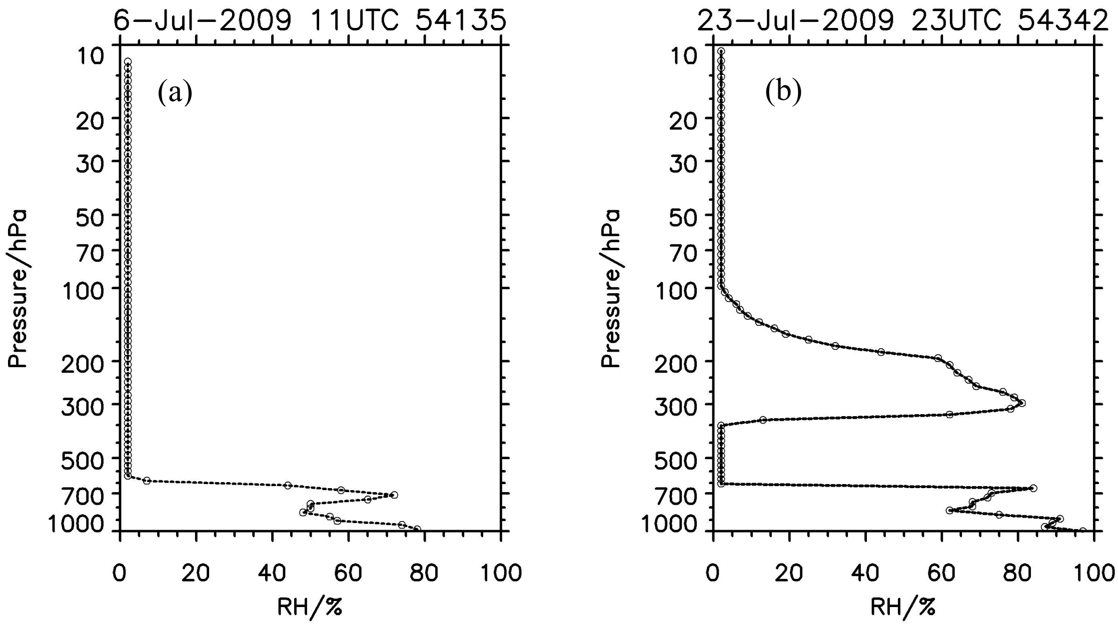

Figure 1. Two typical abnormally dry profile structures of relative humidity observation of the Chinese L-band radiosonde system (From Tang et.al.，2014)

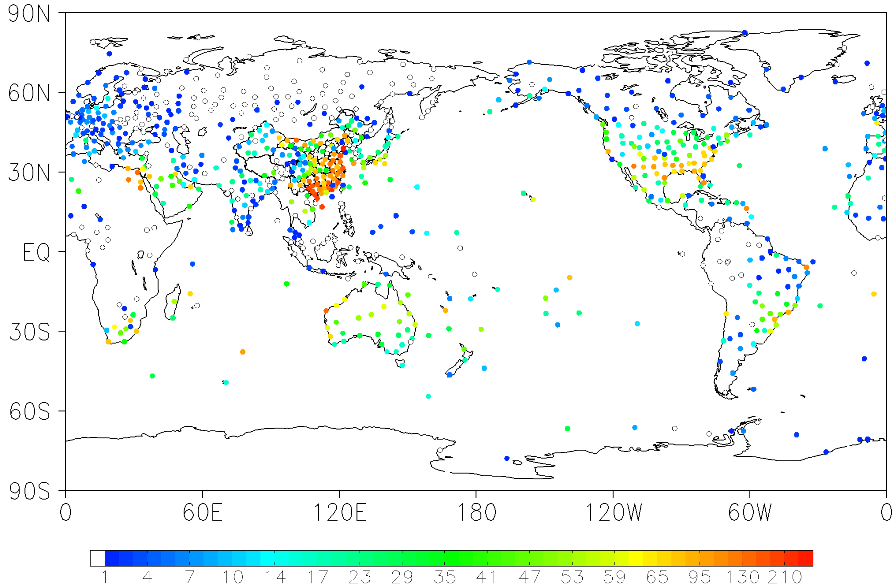

Figure 2. The total number of the failure relative humidity observations for each operational radiosonde station during December 2008 and November 2009. The colour dots correspond to the different number in the colour bar, and the black hollow circle denotes no humidity sensor failure observation.

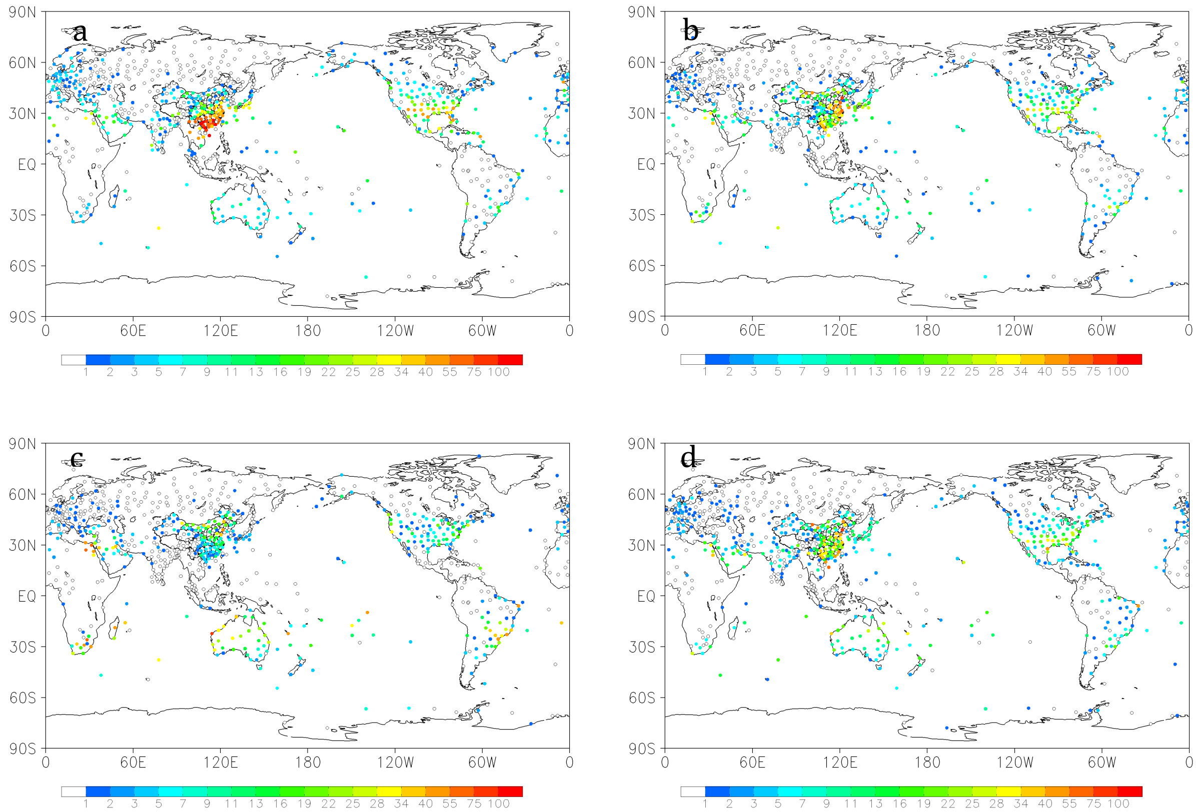

Figure 3. The Same as Figure 2 but for four seasons. Figure 3a-d represent for DJF (December, January and February), MAM (March, April and May), JJA(June, July and August) and SON (September, October and November), respectively.

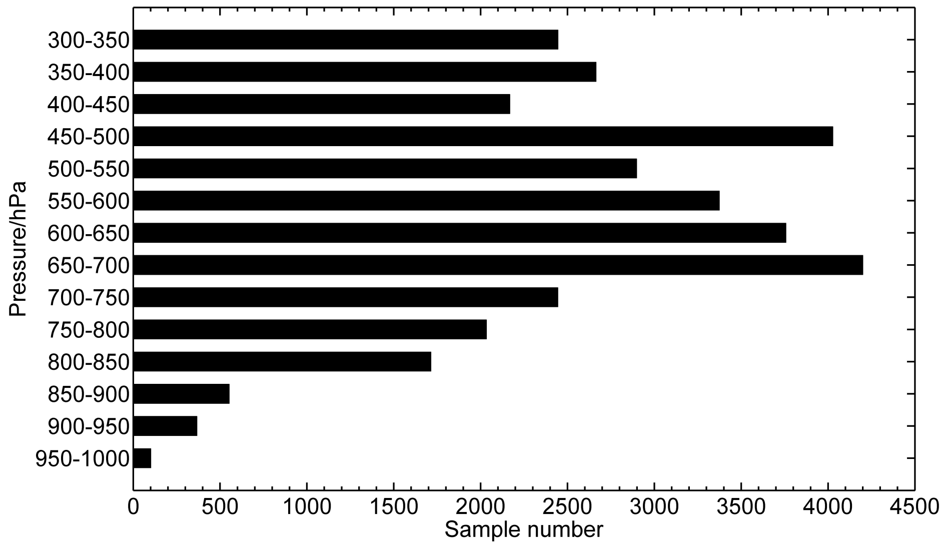

Figure 4. The vertical distribution character of the failure relative humidity observations during December 2008 and November 2009. The x-axis represents the number of relatively humidity observations, and the y-axis presents the height with unit of hPa.

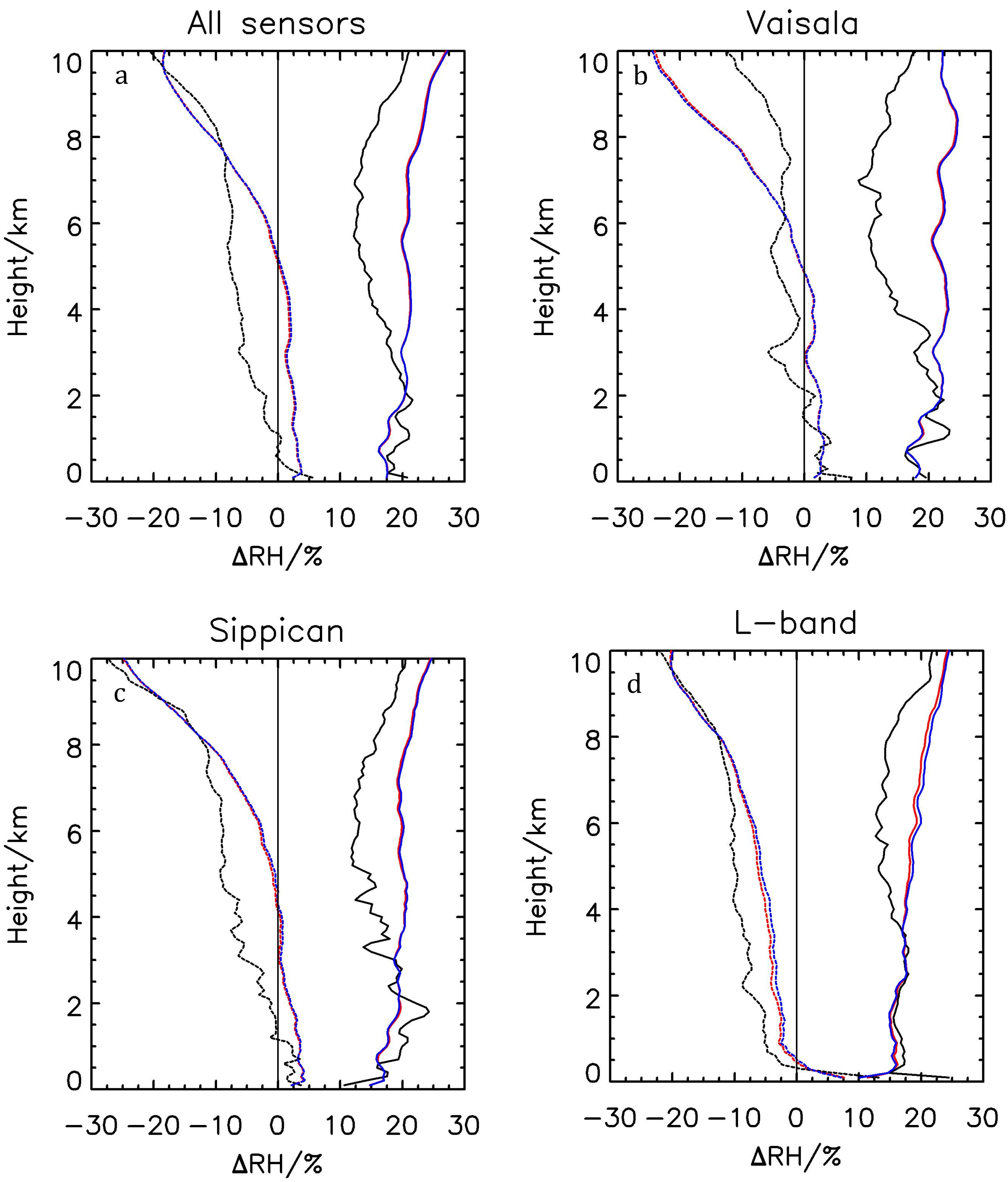

Figure 5. Bias (dashed) and standard deviation (solid) of the relative humidity data between the radiosonde observations and the COSMIC RO retrievals. The red lines represent all observations (not distinguish normal and abnormal observations), the blue lines represent the normal observations, and the black lines represent the false observations. Figure 5a-b are the statistics for all data, Finland Vaisala, USA Sippican and China L-band radiosonde observation.

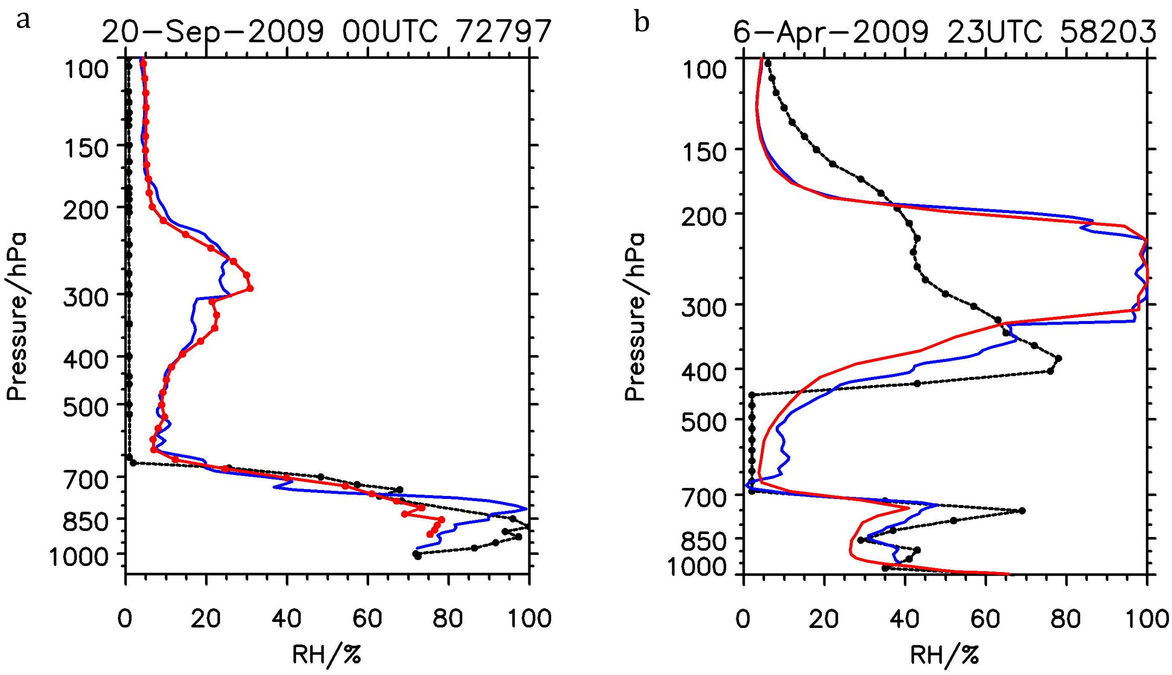

Figure 6. Comparison of the relative humidity profiles among the radiosonde (black), the COSMIC retrieval (blue) and ECMWF reanalysis (red). Figure 6a represents the observation of station 72797 at 00:00:00UTC 20 September 2009； and figure 6b represents the observation of station 58203 at 23:16:41UTC 6 April 2009. The blue(red) lines represent the retrievals(reanalysis) matching the time and space criteria with the radiosonde observation.

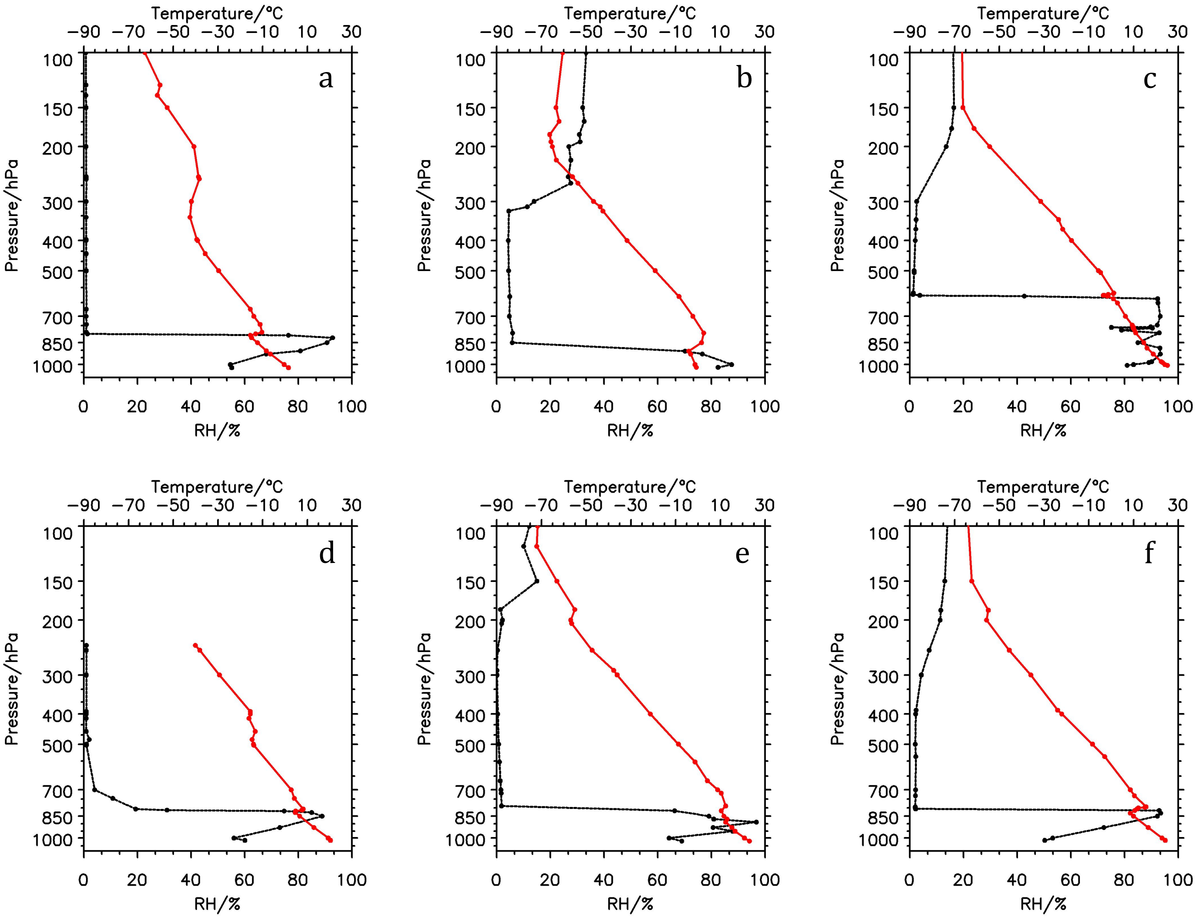

Figure 7. Relative humidity (black) and temperature (red) profiles for different types of radiosonde sensor. Figure 7a-f are cases from Germany Graw Radiosonde G (station 47185 at 12:00:00UTC on 14 January 2009), Russia Meteorit MARZ2-type 2 (station 34247 at 00:00:00UTC on 26 October 2009), American VIZ-B2 (station 78988 at 12:00:00UTC on 17 December 2008), Japan's Meisei RS-016 (station 47991 at 12:00:00UTC on 7 February 2009), Finland Vaisala RS92 (station 83746 at 12:00:00UTC on 21 May 2009) and US Sippican MARK II (station 78526 at 12:00:00UTC on 10 March 2009).

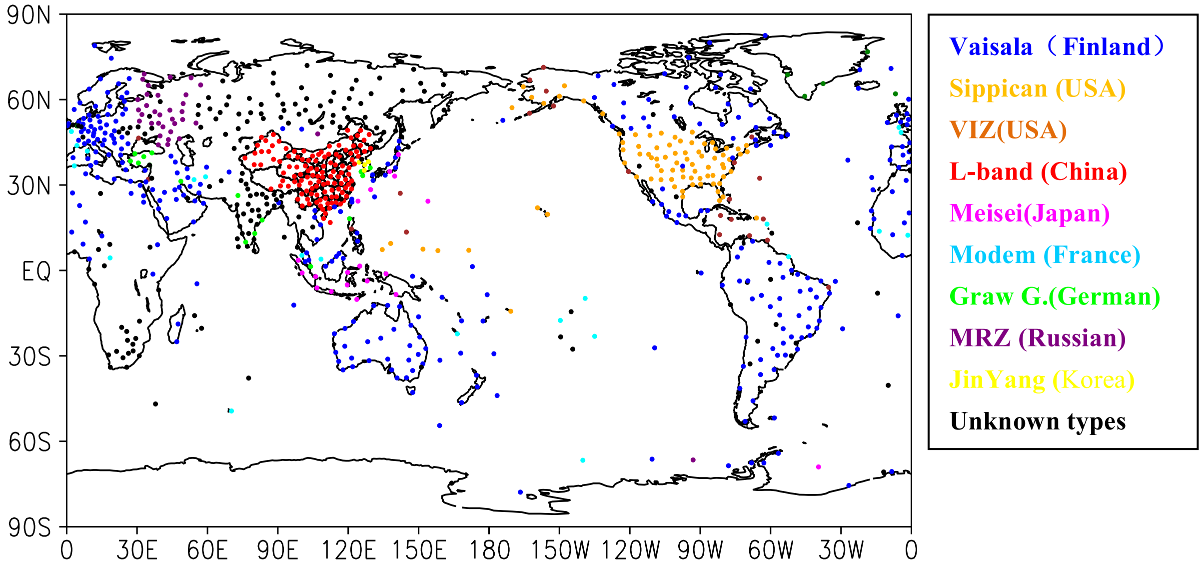

Figure 8. Distribution of the mainly operational radiosonde sensors.

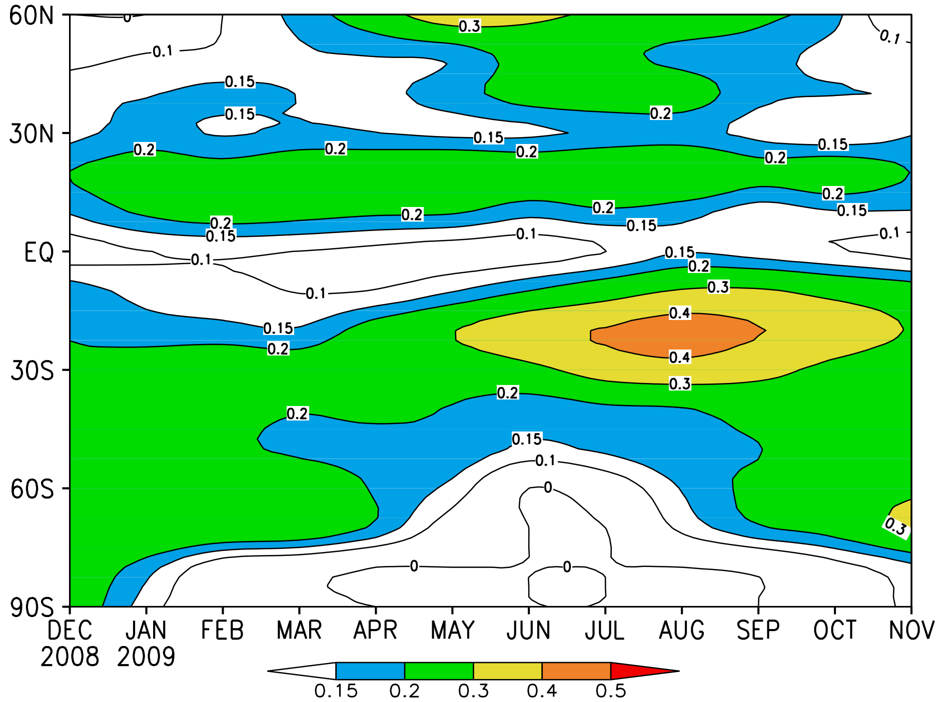

Figure 9. The average longitudinal distribution of stratiform clouds and its temporal evolvement during December 2008 and November 2009.

Table 1. Statistics of total and failure relative humidity observations.

	global		low-latitudes		mid-latitudes of NH		mid-latitudes of SH	
Season	Total	Failure (radio)	Total	Failure(radio)	Total	Failure(radio)	Total	Failure(radio)
DJF （200812-200902）	109592	5996（5.47%）	13748	734(5.34%)	48345	4609(9.53%)	7327	363(4.95%)
MAM （200903-200905）	111496	4402(3.95%)	14040	332(2.36%)	48905	3374(6.90%)	7492	503(6.71%%)
JJA （200906-200908）	112174	3837(3.42%)	15242	572(3.75%)	48863	1852(3.79%)	7242	1218(16.82%)
SON （200909-200911）	113100	4374(3.87%)	15824	499(3.15%)	49442	3070(6.21%)	6654	563(8.46%)
One year （200812-200911）	446362	18609(4.17%)	58854	2137(3.63%)	195555	12905(6.60%)	28715	2647(9.22%)

Table 2. Statistics of all and failure relative humidity observations matched with COSMIC data for different sensors during December 2008 and November 2009.

Sensor	all observations		failure observations	
	total	matched	total (ratio)	matched
All sensors	447021	26405	18609（4.17%）	904
Vaisala	144668	8586	5114（3.53%）	262
Sippican	59607	3670	3347（5.62%）	191
L-band	61736	2657	7796（12.63%）	321